Biosensors and Bioelectronics 24 (2009) 2149–2154

Contents lists available at ScienceDirect

Biosensors and Bioelectronics

journal homepage: www.elsevier.com/locate/bios

# Hydrogen peroxide biosensor based on the direct electrochemistry of myoglobin immobilized on silver nanoparticles doped carbon nanotubes film

Chuan-Yin Liu [a,b], Ji-Ming Hu [a,*]

[a] College of Chemistry and Molecular Sciences, Wuhan University, Wuhan 430072, PR China
[b] Department of Chemistry, Yunyang Teachers College, Danjiangkou 442700, China

ARTICLE INFO

*Article history:*
Received 9 August 2008
Received in revised form 20 October 2008
Accepted 11 November 2008
Available online 18 November 2008

*Keywords:*
Hydrogen peroxide
Myoglobin
Biosensor
Silver nanoparticles doped carbon nanotubes

ABSTRACT

A novel $H_2O_2$ biosensor has been fabricated based on the direct electrochemistry and electrocatalysis of myoglobin (Mb) immobilized on silver nanoparticles doped carbon nanotubes film with hybrid sol–gel techniques. A pair of redox peaks with peak separation of 160 mV and formal potential of −0.295 V was observed at this composite film, corresponding to the direct electrochemistry of Mb. The heterogeneous rate constant was estimated to be 0.41 $s^{-1}$. Under optimum conditions, the amperometric determination of $H_2O_2$ was performed with a linear range of $2.0 \times 10^{-6}$–$1.2 \times 10^{-3}$ mol $L^{-1}$ and a detection limit of $3.6 \times 10^{-7}$ mol/L (S/N = 3). The Michealis–Menten constant was also estimated to be 1.62 mmol $L^{-1}$. The proposed biosensor showed favorable reproducibility, stability, selectivity and accuracy, and has been used to determine $H_2O_2$ in real samples with favorable recoveries.



## 1. Introduction

Biosensors are presently the focus of extensive research for the development of a wide variety of applications in clinical diagnosis, food technology, military, biomedical, industrial and environmental monitoring (Sharma and Rogers, 1994). Two aspects, which are the most problematic in developing protein or enzyme-based biosensors, are the incorporation of sensing molecules in suitable matrix and monitoring the interactions between the analytes and those molecules. So the development of active layers or suitable matrix to immobilize redox proteins for biosensors is an important task (Gooding et al., 2003). In the field of electrochemical biosensors, efforts have been made in designing efficient bio-immobilization matrices as well as improving transduction processes. Acceleration of direct electron transfer between the native redox protein and the underlying electrode is significantly important because it not only provides models for mechanism study of biological electron transport but also enables to construct the mediator-free biosensors and bioreactors (Armstrong and Wilson, 2000). However, the direct electron transfer of redox proteins is very difficult at conventional electrodes, because of the redox centre of proteins being embedded in polypeptide chain structures and the proteins easily being absorbed on the surface of solid electrodes (Victor and Ovadia, 1993). In addition, the retention of the bioactivity of the proteins should be considered. In these circumstances, an important object for biochemists is to achieve efficient electrical contact between the protein and the electrode surface.

Nanomaterials have been used extensively in the fields of physical, chemical and material sciences in the past few years. Carbon nanotubes (CNTs), since its first discovery by Iijima (Iijima, 1991), have gained considerable research interest. CNTs-modified electrodes have shown excellent electrocatalytic activity towards some electroactive substances as $H_2O_2$ due to the fast electron transfer ability of CNTs (Wang, 2005). A dramatic decrease in the overvoltage of $H_2O_2$ was observed with improved sensitivity, which makes the CNTs-modified electrodes of great promise for oxidase-based amperometric biosensors. Nanosized dispersions of metals have also received considerable attention because of their sized-dependent electrical, chemical and optical properties. The electrochemical and catalytic activity of highly dispersed metal nanoparticles is of keen interest in the fabrication of amperometric biosensors (Di et al., 2005). However, aggregation of nanoparticles prohibits the extensive application of the particles. To circumvent this problem, many successful methods have been reported for the stabilization of metal nanoparticles based on capping by polyelectrolytes, or ligands or stabilized in silicate-based matrix. Recently, the research interest has extended to modify CNTs with other nanomaterials so as to optimize the usage of them in various applications. Some nanoparticles have been successfully introduced onto CNTs, such as $TiO_2$ (Banerjee and Wong, 2002), CdSe (Ravindran et al., 2003), Au (Cao et al., 2008), and B (Deng et al., 2008). Furthermore, the evaluation of electrocatalytic activity

* Corresponding author. Tel.: +86 27 62258931.
*E-mail address:* jmhu@whu.edu.cn (J.-M. Hu).

0956-5663/$ – see front matter © 2008 Elsevier B.V. All rights reserved.
doi:10.1016/j.bios.2008.11.007

of various diameters nanoparticles, and the comparison of different nanocomposites based electrochemical biosensors have been investigated (Ferapoutova, 2004; Merkoci, 2007).

Mb is a kind of heme-contained redox proteins and it is also reported that Mb can be used as a substitute of horseradish peroxidase (HRP) to catalyze the reduction of peroxide hydrogen (Liu et al., 2005). In order to retain the electrocatalytic activity and further modification onto the electrode surface, various methods have been used to enhance the electron transfer, such as electropolymerization (Zhang and Hu, 2007), sol–gel (Wang et al., 2004; Ray et al., 2005), layer by layer assembly (Jin et al., 2003), covalent-bonded immobilization (Liu and Hu, 2008) and direct embedded biocompatible membrane (Shen et al., 2002). In those methods, considerable attention has been focused on sol–gel techniques. Sol–gel technology involves the fabrication of materials through the hydrolysis and condensation of suitable precursor, such as alkoxysilane, titanate, alumina and zirconia, and provides a unique means to prepare a three-dimensional network suited for the encapsulation of a variety of biomolecules (Gavalas et al., 2001). Furthermore, porous and open frameworks of sol–gel ensure that the analytes can effectively and fast access to the active functionalities immobilized at the interface between electrode and solution, which results in a high sensitivity to the electrochemical response, as most electron transfer processes are diffusion-controlled (Gupta and Chaudhury, 2007). However, the silica sol–gel, which is commonly used, is brittle and low biocompatible. In order to overcome these obstacles, silica-based organic-inorganic hybrids are adopted as attractive composite materials for the fabrication of biosensors (Walcarius et al., 2005). Some polymers are hybridized into a silica sol–gel matrix, such as polyhydroxyle (PVA-g-PVP) (Wang et al., 1998), chitosan (Tan et al., 2005; Li et al., 2008), poly (vinyl alcohol) (Wang et al., 2000), which can effectively avoid the brittleness of pure inorganic sol–gel and the swelling of some pure polymers. The hybrid sol–gel biosensor possesses several advantages, such as high stability, wide potential window, and easy fabrication at room temperature and encapsulation for electrocatalysts and biocatalysts.

To our knowledge, Ag nanoparticles have been electrodeposited and modified onto CNTs, however, the utilization of Ag nanoparticle doped CNTs (SN-CNTs) to immobilize Mb to achieve direct electrochemistry has never been reported. In the present paper, SN-CNTs was self-synthesized and characterized by XRD and SEM. The nanocomposite was used to modify the electrode surface to construct active layers, and then Mb-hybrid silica sol–gel (HSG) was coated onto the active layers. Due to the biocompatibility and synergistic electrocatalysis of SN-CNTs and ideal micro-circumstance of HSG, the direct electrochemistry of Mb was achieved; the strong electrocatalysis towards $H_2O_2$ has been evaluated by cyclic voltammetry and amperometry. The proposed biosensor results in excellent sensitivity, wide linear range, favorable stability and reproducibility, low detection limit and low Michealis–Menten constant.

## 2. Experimental

### 2.1. Chemicals and instruments

Mb (from horse heart), dopamine (DA) and uric acid (UA) were purchased from Sigma–Aldrich (USA), the stock solution of Mb (10 mg/mL) was prepared by dissolving suitable amount of Mb into 0.1 mol $L^{-1}$ phosphate buffer solution (PBS). Chitosan (CS, >95% deacetylation) was obtained from Shanghai Boao Biochemical Reagent Company, 0.5% CS solution was prepared with 0.1 mol/L acetic acid. Ethyl silicate (TEOS), $AgNO_3$, $K_3Fe(CN)_6$, $NaBH_4$, ascorbic acid (AA), $H_2O_2$ (30%) and other chemicals were from Shanghai chemical reagent Co. (Shanghai, China). 0.1 mol/L PBS was prepared by $NaH_2PO_4$ and $Na_2HPO_4$, and the pH value was adjusted by $H_3PO_4$ and NaOH. All the reagents were of analytical reagent and used as received. Carbon nanotubes (CNTs) with 95% purity were obtained from Nanotechnical Institute of Huazhong Normal University (Wuhan, China), and it was pretreated according to the reference procedure with some modifications (Chattopadhyay et al., 2002). The electrochemical cell was bubbled with high purity of argon for 15 min before usage and kept under Ar atmosphere during measurements. Double-distilled water was used throughout.

All the electrochemical experiments were carried out on a CHI 650A electrochemical workstation (Shanghai, China) with conventional three-electrode cell, the modified glassy carbon electrode was used as working electrode, saturated Ag/AgCl electrode as reference and Pt wire electrode as the counter electrode. UV–vis characterization of Mb, Mb-HSG and Mb-SN-CNTs film was performed at UV-2000 spectrometer (Shanghai Tianneng Technical Co. Ltd.). The characterization of CNTs and SN-CNTs was performed at transmission electronic microscopy (TEM, H-600 STEM/EDX PV9100, Japan), JSM-5610LV scanning electronic microscopy (SEM, JEOL, Japan) and X-ray diffractmeter (XRD, D/Max-IIIA, Rigaku Co. Japan).

### 2.2. Preparation of SN-CNTs

1 mg/mL CNTs was prepared by dissolving suitable amounts of CNTs in 0.5% (*W*:*V*) CS under ultrasonic mixing for 30 min to obtain a homogeneous black suspension. 10 mL of the black suspension and 5 mL of 0.1 mol $L^{-1}$ $AgNO_3$ were added into a round-bottom flask under electromagnetic mixing, then 5 mL 0.02 mol/L $NaBH_4$ (newly prepared) was added to the mixture with vigorous stirring and continued to react for another 15 min. Finally, the mixture was centrifugal separation with super-rate centrifugal machine, rinsed with water and dried under the temperature of 80 °C.

### 2.3. Preparation of CS hybrid organic/inorganic silica sol

5 mL 0.5% CS and 5 mL TEOS were added into a container with vigorous mixing, and then it was ultrasonic mixed for another 60 min until a homogeneous solution resulted and was subsequently stored at room temperature for 3 h. And the pH value of sol was adjusted to 5.0 before usage.

For the preparation of Mb-HSG, 100 μL Mb and 100 μL hybrid sol were mixed in a PVC tube under ultrasonic.

### 2.4. Preparation of Mb modified glassy carbon electrode

The glassy carbon electrode (GCE) with 2 mm diameter was polished with 0.3, 0.1 and 0.05 μm $Al_2O_3$ slurry successively, then it was sonicated with 1:1 $HNO_3$, acetone and double-distilled water for 5 min, respectively. An aliquot of 10 μL of SN-CNTs suspension was coated on the GCE with a microsyringe, and the electrode was dried under an infrared lamp, then 10 μL Mb-hybrid sol was coated onto the surface of SN-CNTs modified GCE, stored for 10 h at 4 °C to acquire the composite film-modified GCE (Mb-HSG-SN-CNTs/GCE). For comparison, the Mb-HSG/GCE and Mb-SN-CNTs/GCE were prepared using the same procedure only omitting the step of adding SN-CNTs or HSG, respectively. All resulting electrodes were washed with water and dry stored at 4 °C refrigeratory when not in use.

### 2.5. Electrochemical characterization and measurements

The electrochemical characterization and measurements were performed with modified GCE as working electrode. Cyclic voltammetry was carried out in the potential range from −0.8 V to 0.5 V. Alternative current impedance was performed in 0.1 mol $L^{-1}$ KCl solution containing 1 mmol $L^{-1}$ $Fe(CN)_6^{3-}$. The frequency range

was from 0.01 Hz to $10^5$ Hz, and the applied potential was set at 0.21 V (the formal potential of $Fe(CN)_6^{3-/4-}$). Amperometric measurements were carried at −0.45 V. All the potentials cited in this paper were referred to saturated Ag/AgCl.

## 3. Results and discussion

### 3.1. Characterization of SN-CNTs

As can be seen from this TEM and SEM images (See supplementary files), the diameter of CNTs is about 15–24 nm, and some particles doped CNTs with its diameter range of 20–35 nm were observed in SN-CNTs film. To further investigation of SN-CNTs, XRD has been performed. As can be seen from Fig. 1, in the $2\theta$ range of 20–80°, except for some peaks corresponding to the element carbon, another four peaks position at corresponding $2\theta$ value 38.831, 45.101, 65.320 and 78.145° appeared for SN-CNTs, which were indexed as <1 1 1>, <2 0 0>, <2 2 0> and <3 1 1>, respectively. Comparing the $2\theta$ value with the literature value of pure SN, it could be inferred that the face-central cubic structure of Ag was doped with CNTs, which was the characteristic crystal peak of silver element.

### 3.2. Electrochemical characterization

Cyclic voltammetry and electrochemical impedance spectroscopy are the effective methods to character the modification process of electrode. For the cyclic voltammograms (CVs) of bare GCE, SN-CNTs/GCE and Mb-HSG-SN-CNTs/GCE in 0.1 mol/L KCl solution containing 1 mmol $L^{-1}$ $Fe(CN)_6^{3-}$. A pair of reversible redox peaks with peak separation ($\Delta E_p$) of 70 mV was observed for bare GCE, indicating that there were no substances to block the mass transfer of probe. However, a pair of peaks with increased peak currents and $\Delta E_p$ of 150 mV was observed at SN-CNTs/GCE with large background current, indicating that the effectively electroactive area of GCE has been increased due to the high special surface area of SN-CNTs. For Mb-HSG-SN-CNTs/GCE, the peak current decreased as compared to SN-CNTs/GCE, this may be attributed to the further modification of Mb-HSG onto the electrode surface, and the film blocked the mass transfer of electroactive probe.

For the Nyquist plots of the above three electrodes, a line in almost all frequencies was observed for the bare GCE, indicating a diffusion controlled process was achieved without other substances to hinder the probe from arriving at the electrode surface. However, a semi-cycle in high frequency range was observed for SN-CNTs/GCE and Mb-HSG-SN-CNTs/GCE, and the diameter corresponding to the resistance of charge transfer of Mb-HSG-SN-CNTs/GCE was larger than that of SN-CNTs/GCE, confirming the further modification process of electrode and indicating that the Mb-HSG film can further block the mass transfer of probe to the electrode surface, the electrochemical behavior of probe was controlled by charge transfer in high frequency.

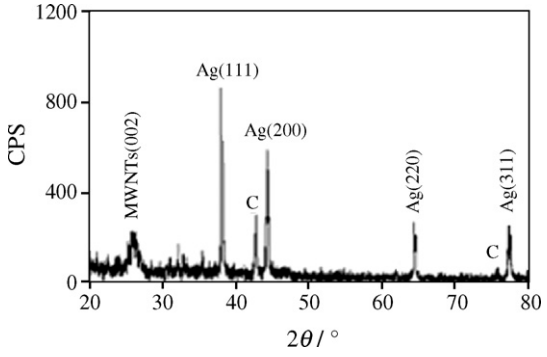


**Fig. 1.** XRD characterization of SN-CNTs.

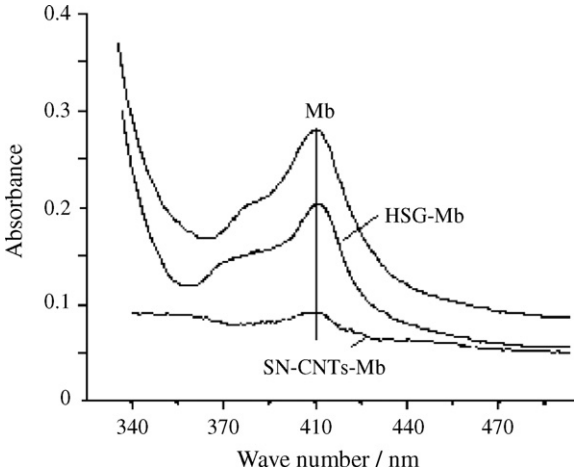


**Fig. 2.** UV–vis spectroscopy of Mb, Mb-HSG and Mb-SN-CNTs film.

### 3.3. UV–vis characterization

UV–vis spectroscopy is a useful tool for monitoring the possible change of the Soret absorption band in the heme group region. The band shift may provide the information of possible denaturation of heme protein particularly that of conformational changes (Chi and Asher, 1998). As can be seen from Fig. 2, an absorption peak was observed at 408 nm for pure Mb film, while lower peaks at 410 nm were observed for Mb-HSG and Mb-SN-CNTs film. There are only 2 nm shifts of absorption peak for Mb-HSG and Mb-SN-CNTs film, indicating that the natural structure of Mb was retained and not denatured.

### 3.4. Direct electrochemistry of Mb

Fig. 3A showed the CVs of Mb-HSG-SN-CNTs/GCE and HSG-SN-CNTs/GCE in deoxygenated PBS. No obvious redox peaks were observed in the potential range of −0.8–0.2 V for HSG-SN-CNTs/GCE, indicating that there were no electroactive substances to react at this range. However, a pair of well-defined symmetrical redox peaks were observed at −0.375 V and −0.214 V with $\Delta E_p$ of 160 mV and formal potential ($E^{\circ\prime} = (E_{pa} + E_{pc})/2$) of −0.295 V for Mb-HSG-SN-CNTs/GCE. Obviously, this pair of redox peaks arose from the redox of the heme Fe centre of Mb embedded in HSG-SN-CNTs film. Yang et al. immobilized Mb and colloidal gold nanoparticles on a GCE by a Nafion film, and a pair of reversible redox peaks appeared with the formal potential of −0.373 V (Yang et al., 2006). Ju et al. immobilized hemoglobin in multi-wall CNTs enhanced grafted collagen matrix and the direct electron transfer of hemoglobin was obtained with formal potential of −0.36 V vs. SCE (Zong et al., 2007). Duan et al. fabricated Mb/MWCNTs/CS film and the direct electrochemistry of Mb with a formal potential of −0.323 V was achieved (Duan et al., 2008). The different formal potential of heme proteins in different system maybe attributed to the effect of different microenvironment on the direct electron transfer.

From Fig. 3B, it can be found that the peak currents increased with increasing of scan rate in 10–400 mV/s, and the cathodic peak currents were linear to scan rate with a regression equation of $I_{pc}(\mu A) = 2.034 + 2.855\,\nu(V/s)$ ($R = 0.9988$). This result indicated that the electrochemical behavior of Mb immobilized on HSG-SN-CNTs film was a surface-controlled process (Bard and Faulkner, 2000). It is also found that peak potential varied

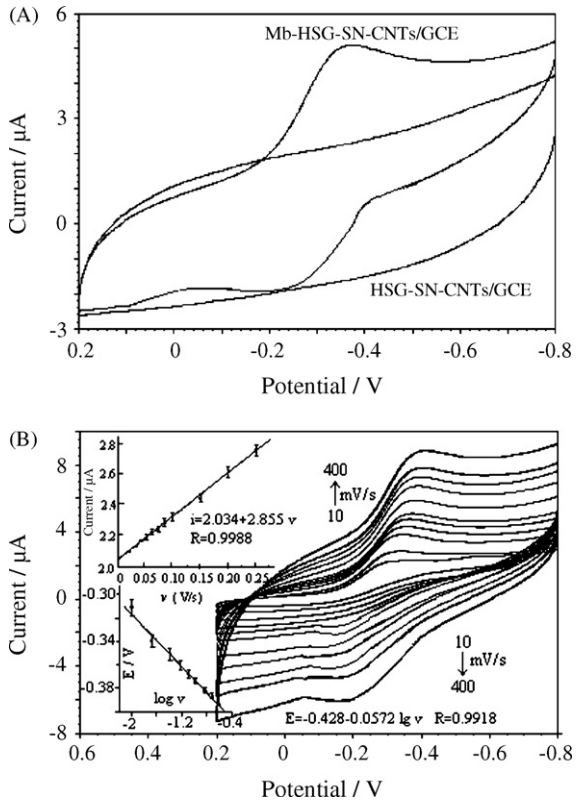


**Fig. 3.** CVs of HSG-SN-CNTs/GCE and Mb-HSG-SN-CNTs/GCE in deoxygenated pH 7 PBS, scan rate: 0.1 V/s (A). CVs of Mb-HSG-SN-CNTs/GCE at different scan rate, the inset figures are the dependence of peak currents vs. scan rate and dependence of potential vs. logarithm value of scan rate (B).

with the scan rate in the range of 10–250 mV/s, while the formal potential kept almost unchanged. The regression equation was $E_{pc} = -0.428 - 0.0572 \log \nu$ with a coefficient of 0.9918. As $n\Delta E_p \leq 200$ mV, the heterogeneous electron transfer rate constant can be estimated by Laviron equation (Laviron, 1979).

$$\log k_s = \alpha \log(1-\alpha) + (1-\alpha)\log\alpha - \log\left(\frac{RT}{nF\nu}\right) - \alpha(1-\alpha)nF\Delta E_p/2.3RT$$

Assuming the electron transfer coefficient is 0.5 and the electron transfer number is 1, in this system, $\Delta E_p$ is 160 mV and scan rate is 0.1 V/s, the rate constant can be estimated to be 0.41 $s^{-1}$. The estimated value is in the controlled range of surface-controlled quasi-reversible process, and is also accord with the values (0.71 $s^{-1}$ and 0.62 $s^{-1}$, respectively) reported elsewhere for heme proteins (Liu and Hu, 2008; Li et al., 2001), indicating that Mb centre $Fe^{III/II}$ underwent a quasi-reversible process.

### 3.5. Optimization of experimental conditions

The pH value of electrolyte will affect the three-dimension extending structure of protein, and will also affect the electrochemical response (Liu et al., 2004). In the pH range of 4.0–9.0, the peak current of Mb-HSG-SN-CNTs/GCE showed linear relationship to pH value of electrolyte. When the pH values were adjusted to below 4.0, the CVs became asymmetric and the cathodic current increased remarkably compared to that obtained at pH values above 4.0. This was likely due to the conformational change of protein in acidic solution. However, in the pH range of 4.0–9.0, the configuration changes are reversible. Once the modified GCE was dipped into pH 7.0 PBS to carry out cyclic voltammetric scan, the symmetrical CVs can be observed again. The phenomena indicated that the configuration changes were related to the $H_2O$ and the protonation of amino acids around the heme group, which was defined as the Redox Bohr Effect (Sun and Wang, 2007). Further investigation of the dependence of peak potential upon pH, it is found that there are linear relationships between peak potential and pH, the regression equations are $E_{pa} = 0.04086 - 0.03707$pH, $R = 0.9951$; $E_{pc} = -0.045 - 0.0452$pH, $R = 0.9994$; $E^{\circ\prime} = 0.002 - 0.0427$ pH, $R = 0.9986$, respectively. This indicated that the effects of protonation of amino acids on the configuration of oxidized state and reduced state were different. The slope of formal potential vs. pH, 42.7 mV/pH, was smaller than theoretical value of 57.6 mV/pH at 18 °C for a single-proton coupled, reversible one-electron transfer (Bond, 1980; Meites, 1965). The reason might be the influence of the protonation states of trans ligands to the heme iron and amino acids around the heme, or the protonation of the water molecule coordinated to the central iron (Yamazaki et al., 1978). As the Mb modified electrode has better electrochemical response at pH 7.0, so all the experiments were performed in pH 7.0 PBS unless specially stated.

The effects of various concentration of CS and different volume ratios of CS and TEOS ($V$:$V$) on the form of sol–gel have also been studied. It is found that the sol–gel had poor mechanical stability with the concentration of CS less than 0.5%, and large background current with the concentration of CS larger than 0.7%. As the concentration of CS was in the range of 0.5–0.7%, better sol–gel properties and higher electrochemical response can be achieved. The HSG had poor mechanical stability with volume ratio less than 1:1 ($V$:$V$). As the content of CS of the sol was steadily increased, the response of the electrode to $H_2O_2$ improved steadily. Composite containing higher than 1:1 resulted in difficulty to construct sol–gel and further influenced the direct electrochemical behavior of Mb entrapped in HSG. Combined with the two aspects, the optimum construction conditions of HSG were selected as 0.5% CS and the ratio of volume ($V$:$V$ = 1:1).

Modification of GCE with different volumes of SN-CNTs was tested for evaluation the electrochemical response of Mb by cyclic voltammetry. As the volume of SN-CNTs increased from 1 μL to 10 μL, the response of electrode improved steadily. As the volumes of SN-CNTs were larger than 10 μL, the response improved slowly with larger background current, which resulted in poor measure for $H_2O_2$. So the optimum loading of SN-CNTs was chosen as 10 μL.

### 3.6. Electrocatalytic activity towards oxygen and $H_2O_2$

The electrocatalytic activity of Mb in this composite film was assessed by cyclic voltammetry and amperometric methods. A pair of well-defined symmetrical redox peaks was observed for Mb-HSG-SN-CNTs/GCE in deoxygenated PBS. When different volumes of air were bubbled into PBS, the cathodic peak increased with anodic peak decreasing. Furthermore, with increasing the volume of air, the cathodic peak current increased and peak potential shifted negatively slightly. This was the characteristic of electrocatalytic reaction of enzyme, indicating that Mb have retained its natural structure and have strong catalytic activity towards oxygen reduction (Andrieux et al., 1980). According to the reference (Hu and Rusling, 1997), the possible mechanism of the reaction can be deduced as below:

$$MbFe^{III} + e \rightarrow MbFe^{II}$$

$$MbFe^{II} + O_2 \rightarrow MbFe^{II}{-}O_2$$

$$MbFe^{II}{-}O_2 + 2e + 2H^+ \rightarrow MbFe^{II} + H_2O_2$$

**Table 1**
Determined value for $H_2O_2$ in real samples (degree of confidence: 90%).

| Real sample | Found by this method (mmol/L) | Found by Fluorescence method (mmol/L) | Added (mmol/L) | Total found (mmol/L) | Recovery (%) |
|---|---|---|---|---|---|
| 1# | 0.256 ± 0.002 | | 0.100 | 0.354 ± 0.003 | 98 |
| 2# | 0.245 ± 0.003 | 0.248 ± 0.003 | 0.100 | 0.348 ± 0.002 | 103 |
| 3# | 0.251 ± 0.002 | | 0.100 | 0.355 ± 0.002 | 104 |

The electrocatalytic activity towards $H_2O_2$ was also evaluated by cyclic voltammetry and amperometric steady-state curves. As can be seen from the CVs of Mb-HSG-SN-CNTs/GCE, Mb-SN/GCE and Mb-CNTs/GCE in different concentration of $H_2O_2$ (See supplementary files), Mb-HSG-SN-CNTs/GCE showed a pair of redox peaks in deoxygenated PBS containing no $H_2O_2$. When Mb-HSG-SN-CNTs/GCE was dipped into PBS containing 0.05 and 0.1 mmol $L^{-1}$ $H_2O_2$, the obvious increase of cathodic peak current was observed; the peak potential appeared at about −0.45 V. Furthermore, the reduction of $H_2O_2$ started at about −0.18 V. Compared with CVs of Mb-SN/GCE and Mb-CNTs/GCE in PBS containing 0.1 mol/L $H_2O_2$, slowly increased cathodic current was observed and the reduction of $H_2O_2$ started at about −0.30 V and −0.28 V, respectively. This is obvious that SN-CNTs have stronger electrocatalytic activity towards $H_2O_2$ than SN and CNTs. It is reported that nanoparicles with diameters of 20–24 nm have better electrocatalytic activity towards $H_2O_2$ (Ferapoutova, 2004; Wang et al., 2003), and nanoparticles modified CNTs have also strong electrocatalytic activity towards analytes (Ding et al., 2007; Wu et al., 2005). In the proposed biosensor, the diameter of SN doped with CNTs was 20–35 nm, combined with the better biocompatibility of SN and CNTs, so the synergistic electrocatalysis of SN-CNTs towards $H_2O_2$ can be obtained.

Amperometric *I–t* curve is the most used method to evaluate the electrocatalytic activity of electrochemical sensors and enzyme-based biosensors. To optimize the suitable applied potential, different potentials have been performed. It is found that the optimum applied potential was −0.45 V for amperometric determination of $H_2O_2$. As expected, large stepwise current was observed with addition of $H_2O_2$ at –0.45 V than that of at −0.6 V (Fig. 4). This is the evidence that Mb embedded in composite film has strong electrocatalytic activity towards $H_2O_2$.

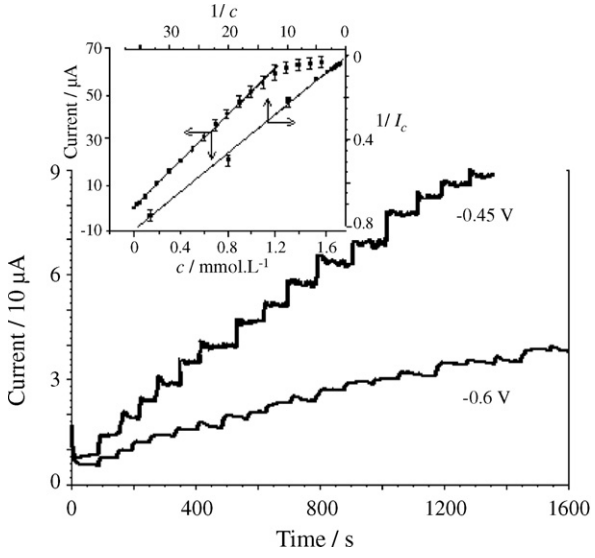


**Fig. 4.** Amperometric *I–t* curves upon successive addition of 0.1 mmol $L^{-1}$ $H_2O_2$ at −0.45 V and −0.6 V. The inset figures are relationship of current vs. conc. of $H_2O_2$ and $1/I_c$ vs. $1/c$.

As can also be seen from the inset figures of Fig. 4, at −0.45 V, the catalytic current is linear to $H_2O_2$ concentration from $2.0 \times 10^{-6}$ to $1.2 \times 10^{-3}$ mol $L^{-1}$, the regression equation is $I_c(\mu A) = 0.278 + 50.83c$ (mmol $L^{-1}$) with a coefficient of 0.999. When the signal to noise is 3, the detection limit is $3.6 \times 10^{-7}$ mol/L. Once the concentration of $H_2O_2$ is larger than 1.3 mmol $L^{-1}$, a current plateau can be observed, this is the characteristic of enzyme-based catalytic reaction. There is a linear relationship between the reciprocal of current and reciprocal of concentration, the regression equation is $1/I_c$ $(1/\mu A) = 0.014 + 0.0225\ 1/c(1/\text{mmol L}^{-1})$, $R = 0.9985$. The apparent Michaelis–Menten constant ($K_m^{app}$) can be calculated according to Linweaver-Burk equation (Kamin and Willson, 1980)

$$\frac{1}{I_{cat}} = \frac{1}{I_{max}} + \frac{K_m^{app}}{I_{max}c}$$

Here, $I_{max}$ is the maximum current under saturated substrate concentration, $c$ is the concentration of $H_2O_2$, $K_m^{app}$ is the apparent Michealis–Menten constant and $I_{cat}$ is the measured current. According to the intercept and slope of above regression equation, $K_m^{app}$ can be estimated to be 1.62 mmol $L^{-1}$. The value is smaller than 23.85 mmol/L for HRP immobilized in sol–gel-derived ceramic-CNTs nanocomposite film (Chen and Dong, 2007). The smaller value of $K_m^{app}$ of present biosensor indicated that Mb embedded in composite HSG-SN-CNTs film had better affinity towards $H_2O_2$ and Mb retained its natural structure and not denatured.

### 3.7. Stability and reproducibility

The reproducibility of the composite film electrode was also studied electrochemically. When the electrode was successfully scanned for 100 cycles, no obvious changes appeared in the CVs. The relative standard deviation (RSD) of peak currents was 2.4% for eleven successfully measurements. Under the optimum conditions, three electrodes were fabricated independently, showed an acceptable RSD of 6.8% for the current determination in presence of 0.1 mmol/L $H_2O_2$. The long-term storage stability of the composite electrode was studied over a certain period of time by monitoring the current to the injection of 0.1 mmol/L $H_2O_2$ with intermittent usage (every 3 days). The composite electrode retained its activity about 91% of its initial value after 30 days and about 78% after 50 days. The better long-term stability could be attributed to the biocompatibility of SN-CNTs and HSG film providing desirable microenvironment for Mb immobilization.

### 3.8. Anti-interfering activity and real sample analysis

The electrochemical reduction of $H_2O_2$ is often interfered by other substances, such as DA, UA and AA. As for the proposed biosensor, amperometric steady-state curve has also been carried out at −450 mV for successive addition of DA, UA and AA to electrochemical cell, the catalytic current of $H_2O_2$ was used to evaluate the interference of those interfering substances. The amperometric responses of DA, UA and AA were very low as compared to equal amount of $H_2O_2$ at this applied potential. When adding 1.0 mmol $L^{-1}$ AA, UA and DA to PBS containing 0.1 mmol $L^{-1}$ $H_2O_2$, the current response for amperometric determination of $H_2O_2$

increased about 5.25%, 3.78% and 2.46%, respectively. The results also indicate that the biosensor has better selectivity.

As the proposed biosensor have better selectivity, reproducibility and stability, the real sample analysis for $H_2O_2$ by the present electrode has been carried out. The real sample (disinfector) was from Hubei Dangjiangkou 1st Hospital, and 10 mL of real sample was added into pH 7 PBS to synthesize the working solution, and also the accurate concentration of $H_2O_2$ has been determined to be 0.248 mmol $L^{-1}$ by fluorescence method. As seen from Table 1, the determined value by this proposed method is very similar to that by fluorescence method, and the recoveries were in the range of 98%–105%.

## 4. Conclusions

In this present paper, a novel $H_2O_2$ biosensor has been fabricated based on immobilization of Mb on composite HSG-SN-CNTs film. The direct electrochemistry of Mb has been achieved with $\Delta E_p$ of 160 mV and formal potential of −0.295 V; the electron transfer rate constant was estimated to be 0.41 $s^{-1}$. The proposed biosensor has been used to determine $H_2O_2$ by amperometry, the linear range was $2.0 \times 10^{-6}$–$1.2 \times 10^{-3}$ mol $L^{-1}$ with a detection limit of $3.6 \times 10^{-7}$ mol $L^{-1}$ (S/N = 3), $K_m^{app}$ was estimated to be 1.62 mmol $L^{-1}$. The present biosensor has favorable reproducibility, stability, selectivity and accuracy.

## Appendix A. Supplementary data

Supplementary data associated with this article can be found, in the online version, at doi:10.1016/j.bios.2008.11.007.

## References


Andrieux, P., Blocman, C., Dumas-Bouchiant, J.M., Saveant, J.M., 1980. J. Electroanal. Chem. 113, 19.
Armstrong, F.A., Wilson, G.S., 2000. Electrochim. Acta 45, 2623–2645.
Banerjee, S., Wong, S.S., 2002. Nano. Lett. 2, 195–200.
Bard, A.J., Faulkner, L.R., 2000. Electrochemical Methods: Principles and Applications. John Wiley and Sons, New York.
Bond, A.M., 1980. Modern Polarographic Methods in Analytical Chemistry. Marcel Dekker, New York.
Cao, W., Wei, C.M., Hu, J.B., Li, Q.L., 2008. Electroanalysis 20, 1925–1931.
Chattopadhyay, D., Galeska, I., Papadimitrakopoulos, F., 2002. Carbon 40, 985–988.
Chen, H.J., Dong, S.J., 2007. Biosens. Bioelectron. 22, 1811–1815.
Chi, Z.H., Asher, S.A., 1998. Biochemistry 37, 2865–2872.
Deng, C.Y., Chen, J.H., Chen, X.L., Xiao, C.H., Nie, L.H., Yao, S.Z., 2008. Biosens. Bioelectron. 23, 1272–1277.
Di, J.W., Shen, C.P., Peng, S.H., Tu, Y.F., Li, S.J., 2005. Anal. Chim. Acta 533, 196–200.
Ding, Y.F., Jin, G.P., Yin, J.G., 2007. Chin. J. Chem. 25, 1094–1098.
Duan, L.S., Xu, Q., Xie, F., Wang, S.F., 2008. J. Electrochem. Sci. 3, 118–124.
Ferapoutova, E.E., 2004. Electroanalysis 16, 1101–1112.
Gavalas, V.G., Andrews, R., Bhattacharyya, D., Bachas, L.G., 2001. Nano. Lett. 1, 719–921.
Gooding, J.J., Eibowo, R., Liu, J.Q., Yang, W.R., Losie, D., Orbons, S., Mearns, F.J., Shapter, J.G., Hibbert, D.B., 2003. J. Am. Chem. Soc. 125, 9006–9007.
Gupta, R., Chaudhury, N.K., 2007. Biosens. Bioelectron. 22, 2387–2399.
Hu, N.F., Rusling, J.F., 1997. Langmuir 13, 4119–4125.
Iijima, S., 1991. Nature 354, 56–58.
Jin, Y.D., Shao, Y., Dong, S.J., 2003. Langmuir 19, 4771–4777.
Kamin, R.A., Willson, G.S., 1980. Anal. Chem. 52, 1198–1205.
Laviron, E., 1979. J. Electroanal. Chem. 101, 19–28.
Li, Q., Luo, G., Feng, J., 2001. Electroanalysis 13, 359–363.
Li, W.J., Yuan, R., Chai, Y.Q., Zhou, L., Chen, S.H., Li, N., 2008. J. Biochem. Biophys. Methods 70, 830–837.
Liu, C.Y., Hu, J.M., 2008a. Chin. Chem. Lett. 19, 955–958.
Liu, C.Y., Hu, J.M., 2008b. Electroanalysis 20, 1067–1072.
Liu, H.H., Tian, Z.Q., Lu, Z.X., Zhang, Z.L., Zhang, M., Pang, D.W., 2004. Biosens. Bioelectron. 20, 294–304.
Liu, Y., Wang, M., Zhao, F., Guo, Z., Chen, H., Dong, S., 2005. J. Electroanal. Chem. 581, 1–10.
Meites, L., 1965. Polarographic Techniques, 2nd ed. Wiley, New York.
Merkoci, A., 2007. Electroanalysis 19, 739–741.
Ravindran, S., Chaudhary, S., Colburn, B., Ozkan, M., Ozkan, C.S., 2003. Nano. Lett. 3, 447–453.
Ray, A., Feng, M.L., Tachikawa, H., 2005. Langmuir 21, 7456–7460.
Sharma, A., Rogers, K.R., 1994. Meas. Sci. Technol. 5, 461–472.
Shen, L., Huang, R., Hu, N.F., 2002. Talanta 56, 1131–1139.
Sun, Y.X., Wang, S.F., 2007. Bioelectrochemistry 71, 172–179.
Tan, X.C., Li, M.J., Cai, P.X., Luo, L.J., Zou, X.Y., 2005. Anal. Biochem. 337, 111–120.
Victor, G., Ovadia, L., 1993. J. Am. Chem. Soc. 115, 2533–2534.
Walcarius, A., Mandler, D., Cox, J.A., Collinson, M., Lev, O., 2005. J. Mater. Chem. 15, 3663–3689.
Wang, B., Li, B., Deng, Q., Dong, S., 1998. Anal. Chem. 70, 3170–3174.
Wang, B., Zhang, J., Cheng, G., Dong, S., 2000. Anal. Chim. Acta 407, 111–118.
Wang, J., 2005. Electroanalysis 17, 7–14.
Wang, Q.L., Lu, G.X., Yang, B.J., 2004. Langmuir 20, 1342–1347.
Wang, G., Xu, J.J., Chen, H.Y., Lu, Z.H., 2003. Biosens. Bioelectron. 18, 335–343.
Wu, Y.Y., Liang, H.P., Hu, J.S., Jiang, L., Wan, L.J., 2005. J. Phys. Chem. B 109, 22212–22216.
Yamazaki, C.I., Araiso, T., Hayashi, Y., Yamada, H., Makino, R., 1978. Adv. Biophys. 11, 249–281.
Yang, W.W., Li, Y.C., Bai, Y., Sun, C.Q., 2006. Sensors Actuators B: Chem. 115, 42–48.
Zhang, H., Hu, N.F., 2007. J. Phys. Chem. B 111, 10583–10590.
Zong, S.Z., Cao, Y., Ju, H.X., 2007. Electroanalysis 19, 841–846.